Quantum Interference Control of Ballistic Pure Spin Currents in Semiconductors

Martin J. Stevens and Arthur L. Smirl*
Laboratory for Photonics & Quantum Electronics, 138 IATL, University of Iowa, Iowa City, Iowa 52242

R. D. R. Bhat, Ali Najmaie, J. E. Sipe, and H. M. van Driel
Department of Physics, University of Toronto, 60 St. George Street, Toronto, Ontario, Canada M5S 1A7
(Received 19 November 2002; published 4 April 2003)

We demonstrate all-optical quantum interference injection and control of a ballistic pure spin current (*without* an accompanying charge current) in GaAs/AlGaAs quantum wells, consisting of spin-up electrons traveling in one direction and spin-down electrons traveling in the opposite direction. This current is generated through quantum interference of one- and two-photon absorption of ~100 fs phase-locked pulses that have orthogonal linear polarizations. We use a spatially resolved pump-probe technique to measure carrier movement of ~10 nm. Results agree with recent theoretical predictions.

DOI: 10.1103/PhysRevLett.90.136603 PACS numbers: 72.25.Dc, 42.65.–k, 72.25.Fe

Spin is one of the fundamental quantum mechanical properties and defining characteristics of electrons and holes in semiconductors. Recently, it has been realized that a deeper understanding and more complete control of spin could lead to the development of novel data processing and storage schemes and, perhaps, ultimately a quantum computer [1]. This interest has led to considerable work on producing spin-polarized currents in semiconductors. Recent studies include demonstrations of incoherent electrical [1] and Zener tunneling [2,3] injection from magnetic semiconductors, incoherent electrical and tunneling injection from ferromagnetic metals [1], and ballistic injection from scanning tunneling microscopes [1]. Moreover, spin-polarized carrier populations produced in semiconductors by the absorption of circularly polarized light have been pulled by external electric fields to create spin-polarized electrical currents [1]. Additionally, several techniques have been employed [4–6] to achieve direct optical injection of spin currents without an external field. In each of these previous demonstrations [1–6], a *net* charge current accompanied the spin current.

In this Letter, by contrast, we report direct optical injection of a spin current that is *not* accompanied by a net charge current. We refer to this as a *pure* spin current. Specifically, we use the quantum mechanical interference between the probability transition amplitudes associated with the one- and two-photon absorption of orthogonally polarized harmonic pulses to generate the pure spin current. Furthermore, we demonstrate that the direction and magnitude of this pure spin current can be controlled by the polarizations and relative phases of the optical pulses.

The geometry that we consider is shown schematically in Fig. 1(a). Two optical pulses, with frequencies ω and 2ω, are incident on a direct gap semiconductor. Their photon energies satisfy the relation $\hbar\omega < E_g < \hbar 2\omega < E_{SO}$, where E_g (E_{SO}) is the heavy-hole (split-off) valence-to-conduction band energy gap, so the ω and 2ω pulses acting independently would generate carriers through two- and one-photon absorption, respectively. These two pulses propagate in the $+z$ direction and have orthogonal linear polarizations, with the ω beam polarization along the x axis and the 2ω beam polarization along the y axis, as shown. For this polarization configuration, Bhat and Sipe [7] recently predicted that there should be no net spin injected and no *net* charge current injected. However, Bhat and Sipe also predicted that this null charge current is actually composed of two equal, but oppositely traveling, spin-polarized currents, as depicted in Fig. 1(a). As shown, quantum interference is expected to produce a current traveling in the $+x$ direction with electron spins oriented in the $-z$ direction ($\mathbf{J}_{+x}^{-z}$) and a current with equal magnitude traveling in the $-x$ direction with spins along $+z$ ($\mathbf{J}_{-x}^{+z}$). The injection rates for these two spin currents traveling along x are given by [7,8]

$$\dot{\mathbf{J}}_{\pm x}^{\mp z} = \pm \dot{J}_1 \cos(\Delta\phi)\hat{\mathbf{x}}, \tag{1}$$

where $\Delta\phi \equiv 2\phi_\omega - \phi_{2\omega}$ and ϕ_ω ($\phi_{2\omega}$) is the phase of the

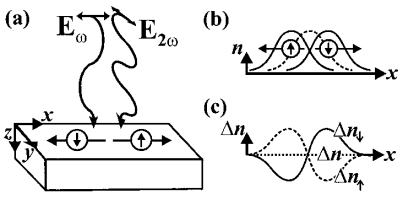

FIG. 1. (a) Geometry for producing a pure spin current using x and y polarized ω and 2ω fields, respectively. Small arrows inside spheres show the direction of net electron spin polarization, while the larger arrows intersecting the spheres show the direction of ballistic electron propagation. Holes (not shown) travel in the directions opposite of their corresponding electrons. (b) Schematic representation of the initial electron distribution (dashed Gaussian profile) and the subsequent motion of the spin-down (spin-up) electrons in the $+x$ ($-x$) direction, yielding no net charge current. (c) The corresponding change in spin-up, spin-down, and total electron densities resulting from this motion.

ω (2ω) beam. The details of $\dot{J}_1$ can be deduced from Ref. [7] (although a different notation is used); however, it is sufficient to note that $\dot{J}_1$ is proportional to $E_\omega^2 E_{2\omega}$ (where E_ω and $E_{2\omega}$ are the fundamental and second harmonic field amplitudes, respectively) and is a function of material parameters, but is independent of $\Delta\phi$.

The sum of the two charge currents represented by Eq. (1) is *exactly* zero. The direction of the ω pulse polarization determines the direction of the currents in the x-y plane, while the phase difference $\Delta\phi$ controls the magnitude and sign of these currents. In effect, this quantum interference and control (QUIC) configuration provides a mechanism for "sorting" the spin of electrons, sending spin "up" in one direction and spin "down" in the opposite direction.

The expected behavior of the transverse spin currents is illustrated schematically in Figs. 1(b) and 1(c). Quantum interference between one-photon absorption of the 2ω pump and two-photon absorption of the ω pump produces a roughly Gaussian initial distribution of carriers in the x-y plane. Initially [dashed line in Fig. 1(b)], there are an equal number of spin-up (electron spin vector in the $+z$ direction) and spin-down (electron spin in the $-z$ direction) electrons produced; however, for $\Delta\phi = 0$ the spin-down (spin-up) electrons should have a preferred ballistic momentum in the $+x$ ($-x$) direction. Thus, before momentum is randomized, the spin-down spatial distribution will shift toward $+x$, and the spin-up distribution toward $-x$.

The accompanying changes expected in the spin-down $[\Delta n_\downarrow(x)]$, spin-up $[\Delta n_\uparrow(x)]$, and total $[\Delta n(x)]$ electron densities resulting from these shifts when $\Delta\phi = 0$ are shown in Fig. 1(c). The magnitude of $\Delta n_\downarrow(x)$ $[\Delta n_\uparrow(x)]$ is determined by the net shift of the initial carrier density profile $n_\downarrow(x)$ $[n_\uparrow(x)]$ arising from the spin current in the $+x$ ($-x$) direction. The shift is determined by the effective number of carriers involved in each current, the ballistic velocity of those carriers, and their average momentum relaxation time. The shifts in Fig. 1(b) are greatly exaggerated; for the carrier density ($\sim 4 \times 10^{17}$ cm^3), lattice temperature (80 K), and excess energy ($\sim$ 200 meV) used here, we expect shifts on the order of a few nm. For such small shifts, the magnitude of $\Delta n_\downarrow(x)$ $[\Delta n_\uparrow(x)]$ should be proportional to the spatial derivative of the initial Gaussian-shaped carrier profile, $\partial n_\downarrow(x)/\partial x$ $[\partial n_\uparrow(x)/\partial x]$.

Because the magnitudes of $\Delta n_\downarrow(x)$ and $\Delta n_\uparrow(x)$ depend on the spin-down and spin-up ballistic currents, respectively, they should also have a cosinusoidal dependence on the phase $\Delta\phi$, as indicated by Eq. (1), so that $\Delta n_\downarrow(x, \Delta\phi) \propto +\cos(\Delta\phi)$ and $\Delta n_\uparrow(x, \Delta\phi) \propto -\cos(\Delta\phi)$. Consequently, when measuring $\Delta n_\downarrow(x, \Delta\phi)$, one expects the signal at each fixed position x to oscillate cosinusoidally with phase $\Delta\phi$. The peak of these oscillations as a function of x should follow the spatial derivative of the initial carrier density. When monitoring $\Delta n_\uparrow(x, \Delta\phi)$ instead of $\Delta n_\downarrow(x, \Delta\phi)$, the phase of the oscillations (as a function of $\Delta\phi$) should flip by π.

Since there is no net charge current, the pure spin current in Eq. (1) cannot be detected with electrodes, as was done in [4,9]. Instead, we use the spatially resolved pump-probe technique depicted in Fig. 2 to monitor the spin separation resulting from these oppositely directed spin-polarized currents. The $\sim$110 fs fundamental pulse, with the wavelength centered at 1.42 μm (the ω beam), is produced by an optical parametric amplifier (OPA) that is pumped by a Ti:sapphire laser-seeded regenerative amplifier operating at 250 kHz. The second harmonic of this pulse at 0.71 μm (2ω) is produced by frequency doubling in a beta barium borate (BBO) crystal. The ω and 2ω pulses are separated using a dichroic beam splitter, and the relative phase between them is controlled with a scanning Michelson interferometer [4,9]. The two pulses, which have orthogonal linear polarizations, are recombined collinearly, overlapped in time, and focused onto the sample at normal incidence [10].

The positions of carriers produced by the ω and 2ω pump beams are interrogated by a tightly focused time-delayed probe pulse, which can be scanned along the x axis across the region excited by the pumps. The probe pulse (at a wavelength of 0.81 μm) is derived from the output of the regenerative amplifier after it has been used to pump the OPA, and it is incident on the sample at an angle of $\sim 10°$ with respect to normal.

The sample is a multiple quantum well (MQW) consisting of ten periods of 14-nm-wide GaAs wells alternating with 17-nm-thick $Al_{0.3}Ga_{0.7}As$ barriers grown on a (001)-oriented GaAs substrate. The sample is mounted on a glass flat, and the GaAs substrate has been removed by selective etching to permit transmission measurements. All measurements are performed at a temperature of 80 K. At this temperature, the pumps generate carriers with an excess energy $2\hbar\omega - E_g$ of $\sim$200 meV, and the probe is resonant with the heavy-hole exciton transition.

The ω and 2ω pulses are focused to spot widths (full width half maximum) of $\sim$14 μm and $\sim$11 μm,

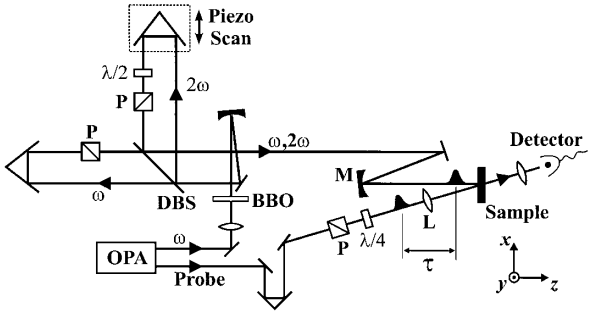

FIG. 2. Experimental geometry for producing and measuring pure spin currents: BBO is used for frequency doubling of ω (1.42 μm) into 2ω (0.71 μm); DBS is a dichroic beam splitter; P, $\lambda/2$, and $\lambda/4$ represent a polarizer, a half wave plate, and a quarter wave plate, respectively; L and M are a lens and a spherical curved mirror with focal lengths of 2 and 5 cm, respectively; τ is the time delay between pumps and probe.

respectively, and the probe to $\sim 6\ \mu$m. The peak irradiances are $\sim 6.7\ \mathrm{GW/cm^2}$ for the ω pulse and $\sim 80\ \mathrm{MW/cm^2}$ for the 2ω pulse. Acting independently, the ω and 2ω pulses each create peak carrier densities (at $x = 0$) of $\sim 2 \times 10^{17}\ \mathrm{cm^{-3}}$ through two- and one-photon absorption, respectively. Data are taken with the probe arriving ~ 4 ps after the pumps to allow the ballistically injected hot carriers to thermalize and the spins of the holes (but not the electrons) to relax [11].

We determine the spin-up and spin-down carrier population at each position by varying the probe polarization and using the circular polarization optical selection rules for excitonic transitions [11–13]. Since the probe is tuned to the heavy-hole excitonic resonance, the change in transmission of a right circularly ($\hat{\boldsymbol{\sigma}}^+$) polarized probe is a measure of spin-down electron density, $n_\downarrow$ (or change in that density, $\Delta n_\downarrow$). Conversely, a left circularly ($\hat{\boldsymbol{\sigma}}^-$) polarized probe is sensitive to $n_\uparrow$ (or $\Delta n_\uparrow$), while a linearly polarized probe is sensitive to the total density, n (or Δn).

Figure 3 illustrates the use of a $\hat{\boldsymbol{\sigma}}^-$ polarized probe to monitor $\Delta n_\uparrow(x, \Delta\phi)$. In Fig. 3(a), the phase-dependent change in probe transmission $\Delta T(\Delta\phi)$ is shown as a function of $\Delta\phi$ for three probe positions along the x axis. For small changes in transmission, $\Delta T(\Delta\phi)$ is proportional to the change in occupancy of the optically coupled states as a function of $\Delta\phi$. Therefore, for a $\hat{\boldsymbol{\sigma}}^-$ probe, $\Delta T(\Delta\phi)$ is a measure of the phase-dependent change in spin-up electron density $[\Delta n_\uparrow(x, \Delta\phi)]$ at a given probe position. The spin-up populations $\Delta n_\uparrow$ at $x \simeq -7.5\ \mu$m and $x \simeq +7.5\ \mu$m both vary sinusoidally with $\Delta\phi$, clearly demonstrating QUIC of the spin-up electrons. The phases of the oscillations at these two positions are expected to differ by π; however, the phase difference shown in Fig. 3(a) deviates from this value by roughly 25%. This deviation is reproducible and is caused by the phase fronts of the ω beam and the 2ω beam not being perfectly parallel. Most importantly, $\Delta n_\uparrow$ at $x \simeq 0$ shows almost no phase dependence. The latter behavior suggests that, for any fixed $\Delta\phi$, an equal number of spin-up electrons move into and out of the probed region.

The peak values of the phase-dependent oscillations shown in Fig. 3(a), together with the peak values at several other probe positions, are plotted as solid circles in Fig. 3(b). Thus, the solid circles in Fig. 3(b) are a measure of the maximum value of the phase-dependent quantity $\Delta n_\uparrow(x, \Delta\phi)$ for several values of x. For comparison, the open squares represent the spatial profile of *all* pump-injected electrons of both spins, $n(x)$, which is independent of phase. This overall density $[n(x)]$ is monitored by using standard synchronous detection techniques to measure the change in probe transmission $\Delta T(n(x))$ with and without the pump pulses present.

Clearly, the peak value of $\Delta n_\uparrow(x, \Delta\phi)$ at each position follows $|\partial n_\uparrow(x)/\partial x| = |\partial n(x)/\partial x|/2$, consistent with our discussion surrounding Figs. 1(b) and 1(c). This derivativelike behavior verifies that we are measuring a QUIC current, as opposed to a QUIC population change. In addition, the contributions from ordinary diffusion are precluded because we have measured only the transmission changes that depend on $\Delta\phi$, and transport arising from diffusion (while present) will be independent of phase. From the relative amplitudes of the solid and dashed curves in Fig. 3(b), we estimate that each of the profiles sketched in Fig. 1(b) moves ~ 10 nm, resulting in a separation of the two spin profiles of ~ 20 nm. If each electron were injected in the x direction with ~ 200 meV of excess energy and if we assume a relaxation time of 45 fs [14], one would expect the separation between spin-up and spin-down electrons to be ~ 90 nm. In actuality, electrons are injected with a distribution of velocities and spin polarizations, so that the expected separation is reduced upon averaging. With these considerations, the measured separation is reasonable.

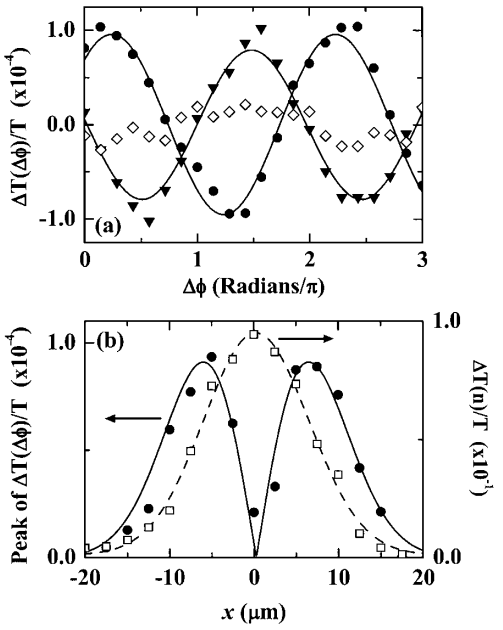

FIG. 3. Phase-dependent differential transmission $[\Delta T(\Delta\phi)]$ vs phase difference $\Delta\phi$, taken with a $\hat{\boldsymbol{\sigma}}^-$ polarized probe at $x \simeq -7.5\ \mu$m (solid triangles), $x \simeq 0$ (open diamonds), and $x \simeq +7.5\ \mu$m (solid circles). Solid lines are sinusoidal fits to the data. (b) Differential transmission as a function of probe position x. The open squares show $\Delta T(n)$, while the solid circles show the peak value of $\Delta T(\Delta\phi)$; these quantities are normalized by transmission through the sample in the absence of the pumps, T, to give $\Delta T(\Delta\phi)/T$ and $\Delta T(n)/T$. The dashed line is a Gaussian fit to $\Delta T(n)/T$, while the solid line is the absolute value of the derivative of that Gaussian.

Figure 4 demonstrates that the currents measured in Fig. 3 are spin polarized and that there is no accompanying charge current. For the data in Fig. 4, the probe position is fixed at $x \simeq +7.5\ \mu$m, and $\Delta T(\Delta\phi)/T$ is measured for three probe polarizations: right circular ($\hat{\boldsymbol{\sigma}}^+$), left circular ($\hat{\boldsymbol{\sigma}}^-$), and linear. Thus, the solid triangles are proportional to $\Delta n_\downarrow(7.5\ \mu\mathrm{m}, \Delta\phi)$, the solid circles to $\Delta n_\uparrow(7.5\ \mu\mathrm{m}, \Delta\phi)$, and the open squares to $\Delta n(7.5\ \mu\mathrm{m}, \Delta\phi)$. The spin-up and spin-down densities

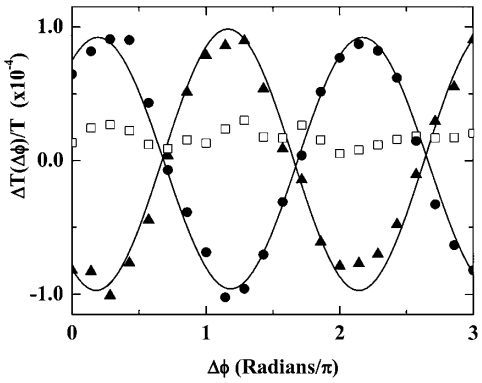

FIG. 4. Phase-dependent differential transmission vs $\Delta\phi$ for three different probe polarizations: $\hat{\boldsymbol{\sigma}}^-$ (solid circles), $\hat{\boldsymbol{\sigma}}^+$ (solid triangles), and linear (open squares), all measured at $x \simeq +7.5$ mm. Solid lines are sinusoidal fits to the data.

are almost exactly π out of phase at this location; therefore, the spin-up and spin-down electrons move in opposite directions for a given $\Delta\phi$, as predicted by Eq. (1). Meanwhile, there is no change in *total* population at this position, which is further evidence there is no net charge current [15].

In summary, the data in Figs. 3 and 4 demonstrate that the quantum mechanical interference between two- and one-photon absorption of ω and 2ω pulses with orthogonal linear polarizations produces a pure spin current that behaves as predicted in Ref. [7]. For a given phase difference between the ω and 2ω pulses, spin-up electrons travel in one direction, while an equal number of spin-down electrons travel in the opposite direction, yielding no net charge current. By controlling this phase difference, we can control the magnitude and sign of the currents.

Finally, we note that we have also investigated QUIC currents produced by two pump pulses with parallel linear polarizations and with the same circular polarizations using the same optical pump-probe techniques described here. We observe characteristics that are consistent with the electrical measurements of these currents that we have reported previously [4] and that are in good agreement with the theoretical predictions of Bhat and Sipe [7]. A detailed description of these measurements is beyond the scope of this Letter and will be presented elsewhere.

We thank Eric Gansen, Scot Hawkins, Petr Nemec, and Yaser Kerachian for insightful conversations. This work was supported in part by the Office of Naval Research, the Defense Advanced Research Projects Agency, Photonics Research Ontario, and the National Science and Engineering Research Council of Canada.

Note added.—We are also pleased to acknowledge that, during the review process, Jens Hübner, Wolfgang Rühle, and co-workers have shared the unpublished results of spatially resolved photoluminescence measurements that provide independent confirmation of the existence of the pure spin currents reported here.

*Electronic address: art-smirl@uiowa.edu

[1] S. A. Wolf, D. D. Awschalom, R. A. Buhrman, J. M. Daughton, S. von Molnár, M. L. Roukes, A. Y. Chtchelkanova, and D. M. Treger, Science **294**, 1488 (2001), and references therein.

[2] M. Kohda, Y. Ohno, K. Takamura, F. Matsukura, and H. Ohno, Jpn. J. Appl. Phys., Pt. 2 **40**, L1274 (2001).

[3] E. Johnston-Halperin, D. Lofgreen, R. K. Kawakami, D. K. Young, L. Coldren, A. C. Gossard, and D. D. Awschalom, Phys. Rev. B **65**, 041306 (2002).

[4] M. J. Stevens, A. L. Smirl, R. D. R. Bhat, J. E. Sipe, and H. M. van Driel, J. Appl. Phys. **91**, 4382 (2002).

[5] S. D. Ganichev, E. L. Ivchenko, S. N. Danilov, J. Eroms, W. Wegscheider, D. Weiss, and W. Prettl, Phys. Rev. Lett. **86**, 4358 (2001).

[6] S. D. Ganichev, E. L. Ivchenko, V.V. Bel'kov, S. A. Tarasenko, M. Sollinger, D. Weiss, W. Wegscheider, and W. Prettl, Nature (London) **417**, 153 (2002).

[7] R. D. R. Bhat and J. E. Sipe, Phys. Rev. Lett. **85**, 5432 (2000).

[8] The theory in [7] was for bulk semiconductors, while quantum wells are used for the measurements reported here. A. Najmaie, R. D. R. Bhat, and J. E. Sipe (private communication) have repeated the calculations in [7] for quantum wells. While there are quantitative differences, the qualitative behavior of the transverse currents in the x-y plane is the same. However, the motion in the longitudinal z direction reported in [7] is restricted in the MQW.

[9] H. M. van Driel and J. E. Sipe, in *Ultrafast Phenomena in Semiconductors*, edited by K.-T. Tsen (Springer-Verlag, New York, 2001), pp. 261–307, and references therein.

[10] Normal incidence excitation prevents qunatum interference control of the overall carrier *population* or *spin*. See J. M. Fraser, A. I. Shkrebtii, J. E. Sipe, and H. M. van Driel, Phys. Rev. Lett. **83**, 4192 (1999).

[11] *Optical Orientation*, edited by F. Meier and B. P. Zakharchenya, Modern Problems in Condensed Matter Sciences Vol. 8 (North-Holland, Amsterdam, 1984).

[12] N. H. Bonadeo, D. G. Steel, and R. Merlin, Phys. Rev. B **60**, 8970 (1999).

[13] S. A. Hawkins, M. J. Stevens, and A. L. Smirl, Phys. Rev. B **64**, 035302 (2001).

[14] P. C. Becker, H. L. Fragnito, C. H. B. Cruz, R. L. Fork, J. E. Cunningham, J. E. Henry, and C.V. Shank, Phys. Rev. Lett. **61**, 1647 (1988).

[15] We also measured the charge current for crossed linear polarizations using charge collection with conventional electrodes (not shown), as was done in Ref. [4], and observed no charge current in the x direction. There was a small charge current in the y direction, but, as predicted by Ref. [7], it was much weaker than the charge current for the same linear or the same circular excitation reported in Ref. [4].